Proceedings of the 9th International Conference on Structural Dynamics, EURODYN 2014
Porto, Portugal, 30 June - 2 July 2014
A. Cunha, E. Caetano, P. Ribeiro, G. Müller (eds.)
ISSN: 2311-9020; ISBN: 978-972-752-165-4

Transition radiation excited by a load moving over the interface of two elastic layers

Karel N. van Dalen[1], Andrei V. Metrikine[1], Apostolos Tsouvalas[1]
[1]Dept. of Structural Engineering, Faculty of Civil Engineering and Geosciences, Delft University of Technology,
Stevinweg 1, 2628 CN Delft, The Netherlands
email: k.n.vandalen@tudelft.nl, a.metrikine@tudelft.nl, a.tsouvalas@tudelft.nl

ABSTRACT: Transition radiation is emitted when a perturbation source (e.g., electric charge, mechanical load), which does not possess an inherent frequency, moves along a straight line at a constant velocity in or near an inhomogeneous medium. The phenomenon was described for the first time in electromagnetics, but it is universal from the physical point of view. Transition radiation of elastic waves is emitted, for example, by a train running on a conventional railway track. The wheels of the train excite elastic waves in the track due to inhomogeneities such as non-uniform subsoil. Transition radiation of elastic waves has been studied in several 1D and 2D elastic systems, but the radiation in an elastic continuum has only been described in an idealized model consisting of two half-planes with constant load that crosses the interface. Nevertheless, the study provided physical insight into the mechanism of transition radiation. Body waves as well as interface waves can be excited, and the radiation spectra of the former show peculiar directivities due to the coupling of the waves at the interface. Here, we describe transition radiation in a more realistic continuum model of two elastic layers with a free surface. The constant load now moves along the free surface and passes over the interface of the two layers. The major difference from the above-mentioned model is the possible radiation of free-surface (Rayleigh) waves. In both layers, the radiation fields consist of a summation of guided modes, and the fields are coupled at the interface. Orthogonality relations derived from the elastodynamic reciprocity theorem are used to find the modal coefficients. Based on the derived solution, the spectra of radiation energy and their directivities can be calculated.

KEY WORDS: Moving load dynamics, transition radiation in elastic continuum, inhomogeneous medium

1 INTRODUCTION

Transition radiation is emitted when a perturbation source (electric charge, acoustic monopole, mechanical load, etc.), which does not possess an inherent frequency, moves along a straight line at a constant velocity in an inhomogeneous medium or near such a medium [1]. This phenomenon was described for the first time by Ginzburg & Frank [2], who analyzed radiation of electromagnetic waves by a charged particle crossing the boundary between an ideal conductor and vacuum. Already in early studies concerned with transition radiation, it was demonstrated that this phenomenon is universal from the physical point of view, meaning that it occurs irrespective of the physical nature of the waves.

The first study on transition radiation of elastic waves was published by Vesnitskii & Metrikine [3]. Such radiation is emitted, for example, by a train running on a conventional railway track. The wheels of the train, pressed against the rails by gravity, excite elastic waves in the railway track due track inhomogeneity caused by sleepers, non-uniform subsoil, etc. A review of the early studies on transition radiation of elastic waves in one- and two-dimensional elastic systems (i.e., strings, beams, membranes and plates) can be found in [4]. Recently, the problem of the beam on inhomogeneous Winkler foundation again attracted attention due to the introduction of some other solution methods (modal summation, moving element method; [5,6]) and the incorporation of non-linear springs aiming at a more realistic description of the track substructure [7]. In addition, transition radiation was explicitly addressed – apart from possibly giving rise to vehicle instability and passenger discomfort – as the physical cause of railroad degradation due to the associated and often strong amplification of the stress and strain fields [8].

Transition radiation of waves in an elastic continuum was first described by van Dalen & Metrikine [9]. The adopted model consists of two elastic half-planes with a constant load that crosses the interface between the half-planes along the path normal to this interface. Though the chosen model has no direct practical application, the study provides physical insight into the mechanism of transition radiation in an elastic continuum. Body (compressional and shear) waves as well as interface waves (i.e., Stoneley waves) can be excited, and the radiation spectra of the former show peculiar directivities, which is due to the coupling of the radiated waves at the interface.

In the current paper, we describe the phenomenon of transition radiation in a more realistic continuum model of two elastic layers having a free surface (i.e., wave guides). The constant load now moves along the free surface and passes over the interface that connects the two layers, see Figure 1. The major difference from the above-discussed continuum model is the possible radiation of surface waves along the free surface (i.e., Rayleigh waves). The current model also requires a different method of solution in which the radiation fields consist of summations of guided modes. The radiation fields in both layers are coupled at the interface. In fact, this constitutes an interaction or coupled problem in which each mode in one layer is coupled to all modes of the other. Orthogonality relations, which are derived from the Rayleigh-Betti elastodynamic reciprocity theorem [10-13] and interrelate the modal eigenfunctions, are employed to find the modal amplitudes. The presented solution can be used to calculate the spectra of radiation energy.

2 MODEL AND SOLUTION

We consider a point load F that moves over the interface of two elastic layers, as shown in Figure 1. The elastic layers have a stress-free surface and are fixed to a rigid bottom. Though we restrict the model to two dimensions, it allows for the existence of body and free-surface waves and is thus appropriate for providing new insights into the mechanism of transition radiation. The velocity of the load is taken sub-critical and constant so that the transition radiation does not interfere with other possible radiation effects (like Mach/Vavilov-Cherenkov radiation); however, the method of solution described in this paper is not restricted to this assumption. Furthermore, we note that we disregard start-up effects of the load.

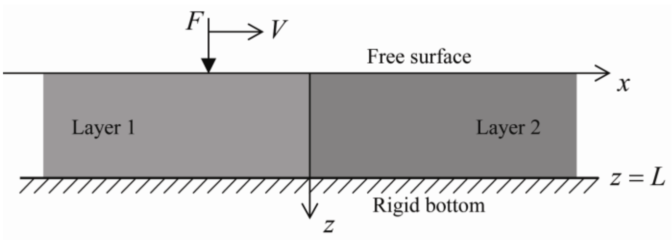

Figure 1: Two-dimensional model of a point load F moving over the interface of two elastic layers at velocity V. The thickness of the layers is L.

The behaviour of the layers is described by the equations of a classical elastic continuum [11-13]. The boundary conditions for the stress $\boldsymbol{\sigma}$ and the displacement $\mathbf{u}$ at the different edges are (superscripts 1 and 2 denote left and right layers, respectively)

$$\begin{aligned} &\sigma_{zz}^{(1)} = \begin{cases} -F\delta\left(x-Vt\right), & t<0, \\ 0, & t \geq 0, \end{cases} \\ &\sigma_{zz}^{(2)} = \begin{cases} 0, & t<0, \\ -F\delta\left(x-Vt\right), & t \geq 0, \end{cases} \\ &\sigma_{zx}^{(1,2)} = 0, \end{aligned} \tag{1}$$

at $z = 0$,

$$u_x^{(1,2)} = 0, \qquad u_z^{(1,2)} = 0, \tag{2}$$

at $z = L$, and

$$\begin{aligned} \sigma_{xx}^{(1)} &= \sigma_{xx}^{(2)}, & \sigma_{xz}^{(1)} &= \sigma_{xz}^{(2)}, \\ u_x^{(1)} &= u_x^{(2)}, & u_z^{(1)} &= u_z^{(2)}, \end{aligned} \tag{3}$$

at $x = 0$; here, x and z are the horizontal and vertical coordinates, respectively, L the thickness of the layer (see Figure 1), t denotes time, and $\delta(...)$ the Dirac delta function.

An analytical solution to the stated problem can be found by splitting it into a steady-state part and a transient part for each of the domains ($x < 0$ and $x > 0$). The steady-state part is the so-called eigenfield of the load that is stationary in the reference system that moves with the load if it moves along a homogeneous layer [4]; this field is confined to the vicinity of the load (due to its sub-critical velocity). The eigenfield changes as the load crosses the interface at $x = 0$, which can be thought of as the source of transition radiation. The transient part of the solution captures the corresponding radiation field that, though excited by the load, propagates independently of it; hence, it is referred to as the free field (or: fields, when explicitly referring to the solutions in both layers). Thus:

$$\begin{aligned} \mathbf{u}^{(i)}\left(x,z,t\right) &= \mathbf{u}^{(i),e}\left(x,z,t\right) + \mathbf{u}^{(i),f}\left(x,z,t\right), \\ \boldsymbol{\sigma}^{(i)}\left(x,z,t\right) &= \boldsymbol{\sigma}^{(i),e}\left(x,z,t\right) + \boldsymbol{\sigma}^{(i),f}\left(x,z,t\right), \end{aligned} \tag{4}$$

where the superscripts "e" and "f" indicate the eigenfield and the free field, respectively, and $i = 1,2$.

The eigenfield of the load can be found by applying the Fourier transform over time and over the horizontal coordinate. Upon applying Helmholtz decomposition, two decoupled ordinary differential equations are obtained that can be solved in a straightforward manner. Then, after applying the inverse Fourier transform over horizontal wavenumber, the following result is obtained:

$$\begin{aligned} \hat{\varphi}^{(i),e} &= \frac{F}{V}\mathrm{e}^{-\mathrm{i}\omega x/V}\left(A_{P1}^{(i)}\mathrm{e}^{+\mathrm{i}q_P^{(i)}(z-L)} + A_{P2}^{(i)}\mathrm{e}^{-\mathrm{i}q_P^{(i)}z}\right), \\ \hat{\psi}^{(i),e} &= \frac{F}{V}\mathrm{e}^{-\mathrm{i}\omega x/V}\left(A_{S1}^{(i)}\mathrm{e}^{+\mathrm{i}q_S^{(i)}(z-L)} + A_{S2}^{(i)}\mathrm{e}^{-\mathrm{i}q_S^{(i)}z}\right), \end{aligned} \tag{5}$$

where $\hat{\varphi}$ and $\hat{\psi}$ denote the Helmholtz potentials for dilatation and rotation, respectively, the hats refer to the space-frequency domain, ω denotes angular frequency, i the imaginary unit, $A_{P1,P2,S1,S1}^{(i)}$ are coefficients determined by the boundary conditions (1) and (2), and the factors in the exponent are defined as

$$q_{P,S}^{(i)} = -\mathrm{i}\frac{|\omega|}{V}\sqrt{1-\left(\alpha_{P,S}^{(i)}\right)^2}, \quad \alpha_{P,S}^{(i)} = \frac{V}{c_{P,S}^{(i)}} < 1. \tag{6}$$

Here, $c_{P,S}^{(i)}$ denote the compressional and shear wave velocities of the two layers. The space-frequency domain displacements and stresses can be obtained from the expressions in Eq. (5) by taking the appropriate derivatives [12].

Now that the eigenfields have been found, the free fields can be determined. Since the eigenfields already account for the presence of the load, the free-field boundary conditions at the upper surface are homogeneous [cf. Eq. (1)], as well as at the rigid bottom:

$$\begin{aligned} &\sigma_{zz}^{(i),f} = 0, \quad \sigma_{zx}^{(i),f} = 0, \quad \text{at} \quad z = 0, \\ &u_x^{(i),f} = 0, \quad u_z^{(i),f} = 0, \quad \text{at} \quad z = L. \end{aligned} \tag{7}$$

Using the known eigenfields, the interface conditions in Eq. (3) can be written in the space-frequency domain as

$$\begin{aligned} &\hat{\sigma}_{xx}^{(1),f} - \hat{\sigma}_{xx}^{(2),f} = \hat{\sigma}_{xx}^{(2),e} - \hat{\sigma}_{xx}^{(1),e} = \Delta\hat{\sigma}_{xx}^{e}, \\ &\hat{\sigma}_{zx}^{(1),f} - \hat{\sigma}_{zx}^{(2),f} = \hat{\sigma}_{zx}^{(2),e} - \hat{\sigma}_{zx}^{(1),e} = \Delta\hat{\sigma}_{zx}^{e}, \\ &\hat{u}_{x}^{(1),f} - \hat{u}_{x}^{(2),f} = \hat{u}_{x}^{(2),e} - \hat{u}_{x}^{(1),e} = \Delta\hat{u}_{x}^{e}, \\ &\hat{u}_{z}^{(1),f} - \hat{u}_{z}^{(2),f} = \hat{u}_{z}^{(2),e} - \hat{u}_{z}^{(1),e} = \Delta\hat{u}_{z}^{e}, \end{aligned} \tag{8}$$

which expresses that the difference in eigenfields is responsible for the generation of transition radiation. The free fields can be expressed in terms of a summation of infinitely many guided wave modes:

$$\begin{aligned} \hat{\varphi}^{(1),f} &= \sum_{k=1}^{\infty} C_k^{(1)} \mathrm{e}^{+\mathrm{i}k_{x;k}^{(1)}x} Z_{P;k}^{(1)}(z), \\ \hat{\psi}^{(1),f} &= \sum_{k=1}^{\infty} C_k^{(1)} \mathrm{e}^{+\mathrm{i}k_{x;k}^{(1)}x} Z_{S;k}^{(1)}(z), \\ \hat{\varphi}^{(2),f} &= \sum_{n=1}^{\infty} C_n^{(2)} \mathrm{e}^{-\mathrm{i}k_{x;n}^{(2)}x} Z_{P;n}^{(2)}(z), \\ \hat{\psi}^{(2),f} &= \sum_{n=1}^{\infty} C_n^{(2)} \mathrm{e}^{-\mathrm{i}k_{x;n}^{(2)}x} Z_{S;n}^{(2)}(z), \end{aligned} \tag{9}$$

where the minus and the plus in the exponent correspond to the left and right layers, respectively, $\mathrm{Im}\left(k_{x;k}^{(1)}, k_{x;n}^{(2)}\right) \le 0$ to comply with the radiation conditions, and

$$\begin{aligned} Z_{P;k}^{(1)}(z) &= B_{P1;k}^{(1)} \mathrm{e}^{+\mathrm{i}k_{z,P;k}^{(1)}(z-L)} + B_{P2;k}^{(1)} \mathrm{e}^{-\mathrm{i}k_{z,P;k}^{(1)}z}, \\ Z_{S;k}^{(1)}(z) &= B_{S1;k}^{(1)} \mathrm{e}^{+\mathrm{i}k_{z,S;k}^{(1)}(z-L)} + B_{S2;k}^{(1)} \mathrm{e}^{-\mathrm{i}k_{z,S;k}^{(1)}z}. \\ Z_{P;n}^{(2)}(z) &= B_{P1;n}^{(2)} \mathrm{e}^{+\mathrm{i}k_{z,P;n}^{(2)}(z-L)} + B_{P2;n}^{(2)} \mathrm{e}^{-\mathrm{i}k_{z,P;n}^{(2)}z}, \\ Z_{S;n}^{(2)}(z) &= B_{S1;n}^{(2)} \mathrm{e}^{+\mathrm{i}k_{z,S;n}^{(2)}(z-L)} + B_{S2;n}^{(2)} \mathrm{e}^{-\mathrm{i}k_{z,S;n}^{(2)}z}. \end{aligned} \tag{10}$$

Throughout the paper, summation over repeated indices is not invoked. The $C_k^{(1)}$ and $C_n^{(2)}$ are modal coefficients to be determined by the interface conditions, $k_{x;k}^{(1)}$ and $k_{x;n}^{(2)}$ are modal horizontal wavenumbers computed from the characteristic equations of the corresponding eigenvalue problems that are formed by substitution of the solutions given by Eq. (9) into the boundary conditions Eq. (7) (i.e., for both layers, a similar eigenvalue problem needs to be solved); the $Z_P^{(i)}(z)$ and $Z_S^{(i)}(z)$ functions are the associated modal eigenfunctions of the potentials whose coefficients $B_{P1,P2,S1,S2}^{(i)}$ are found from the eigenvectors of the eigenvalue problem (modal indices omitted for brevity). The vertical modal wavenumbers are defined as

$$\begin{aligned} k_{z,P;k}^{(1)} &= \sqrt{\left(k_P^{(1)}\right)^2 - \left(k_{x;k}^{(1)}\right)^2}, \\ k_{z,S;k}^{(1)} &= \sqrt{\left(k_S^{(1)}\right)^2 - \left(k_{x;k}^{(1)}\right)^2}, \\ k_{z,P;n}^{(2)} &= \sqrt{\left(k_P^{(2)}\right)^2 - \left(k_{x;n}^{(2)}\right)^2}, \\ k_{z,S;n}^{(2)} &= \sqrt{\left(k_S^{(2)}\right)^2 - \left(k_{x;n}^{(2)}\right)^2}, \end{aligned} \tag{11}$$

where $k_{P,S}^{(i)} = \omega / c_{P,S}^{(i)}$ are the body wavenumbers of the compressional and shear waves, respectively.

In order to determine the unknown modal coefficients, the free-field solution [Eq. (9)] is substituted into the interface conditions [Eq. (8)]:

$$\begin{aligned} &\sum_{k=1}^{\infty} C_k^{(1)} Z_{xx;k}^{(1)}(z) - \sum_{n=1}^{\infty} C_n^{(2)} Z_{xx;n}^{(2)}(z) = \Delta\hat{\sigma}_{xx}^{e}(z), \\ &\sum_{k=1}^{\infty} C_k^{(1)} Z_{zx;k}^{(1)}(z) - \sum_{n=1}^{\infty} C_n^{(2)} Z_{zx;n}^{(2)}(z) = \Delta\hat{\sigma}_{zx}^{e}(z), \\ &\sum_{k=1}^{\infty} C_k^{(1)} Z_{x;k}^{(1)}(z) - \sum_{n=1}^{\infty} C_n^{(2)} Z_{x;n}^{(2)}(z) = \Delta\hat{u}_{x}^{e}(z), \\ &\sum_{k=1}^{\infty} C_k^{(1)} Z_{z;k}^{(1)}(z) - \sum_{n=1}^{\infty} C_n^{(2)} Z_{z;n}^{(2)}(z) = \Delta\hat{u}_{z}^{e}(z), \end{aligned} \tag{12}$$

where the z dependence is included for clarity. The eigenfunctions for stresses and displacements $Z_{xx}^{(i)}$, $Z_{zx}^{(i)}$, $Z_x^{(i)}$ and $Z_z^{(i)}$ (modal indices left out) are obtained by applying the appropriate derivatives to the above-defined eigenfunctions of the potentials. Eq. (12) shows that each wave mode of layer 1 is coupled to all modes of layer 2, and vice versa. Hence, the problem to determine the free fields can be referred to as an interaction or a coupled problem. Now, to derive the coefficients $C_k^{(1)}$ and $C_n^{(2)}$ from Eq. (12), a relation is required that expresses the orthogonality of the different modes for each of the layers:

$$\int_0^L \left(Z_{x;l}^{(i)} Z_{xx;m}^{(i)} - Z_{zx;l}^{(i)} Z_{z;m}^{(i)} \right) dz = N_m^{(i)} \delta_{lm}, \tag{13}$$

where δ_{lm} is the Kronecker delta and $N_m^{(i)}$ is a complex number. This relation can be derived from the reciprocity theorem of the convolution type and thus interrelates the properties of different depth-dependent eigenfunctions in each of the layers [10-13]; it is sometimes referred to as a bi-orthogonality relation [14]. Now, by taking combinations of the interface conditions in Eq. (12) and integrating them over the depth of the layers, the orthogonality relation can be employed. Finally, the following expression is obtained in terms of the coefficients of layer 1 only:

$$C_m^{(1)} - \frac{1}{N_m^{(1)}} \sum_{k=1}^{M_1} C_k^{(1)} \sum_{n=1}^{M_2} \frac{D_{kn} D_{mn}}{N_n^{(2)}} = \frac{1}{N_m^{(1)}} \left(S_{I;m} - \sum_{n=1}^{M_2} \frac{S_{II;n} D_{mn}}{N_n^{(2)}} \right), \tag{14}$$

where M_1 and M_2 represent the finite number of modes in layers 1 and 2 (see explanation below), respectively, and

$$\begin{aligned} D_{km} &= \int_0^L \left(Z_{xx;k}^{(1)} Z_{x;m}^{(2)} - Z_{z;k}^{(1)} Z_{zx;m}^{(2)} \right) dz, \\ S_{I;m} &= \int_0^L \left(\Delta \hat{u}_x^e Z_{xx;m}^{(1)} - \Delta \hat{\sigma}_{zx}^e Z_{z;m}^{(1)} \right) dz, \\ S_{II;n} &= \int_0^L \left(\Delta \hat{\sigma}_{xx}^e Z_{x;n}^{(2)} - \Delta \hat{u}_z^e Z_{zx;n}^{(2)} \right) dz. \end{aligned} \tag{15}$$

Here, D_{km} is a matrix that contains cross multiplications of the eigenfunctions of the two layers, and $S_{I;m}$ and $S_{II;n}$ can be considered as source terms for mode m (in layer 1) and mode n (in layer 2) that depend on the difference in eigenfields of the adjacent layers.

The modal coefficients can be solved for using Eq. (14) by writing it in matrix-vector form and subsequently inverting the obtained equation. This is, however, only possible when a finite number of modes is incorporated in each of the layers, and for this reason truncation was applied in Eq. (14). Once the coefficients of layer 1 have been determined, those of layer 2 can be computed from the following relation:

$$C_n^{(2)} = \frac{1}{N_n^{(2)}} \sum_{k=1}^{M_1} C_k^{(1)} D_{kn} - \frac{S_{II;n}}{N_n^{(2)}}. \tag{16}$$

This concludes the derivation of the free fields. By adding them to the eigenfields according to Eq. (4), the total space-frequency domain solution of the transition radiation problem is obtained.

3 NUMERICAL RESULTS

In this section, we give some preliminary results to show that obtained analytical solution satisfies the interface conditions given by Eq. (8). Approximate solutions will not satisfy the interface conditions exactly, which possibly gives rise to inaccuracies in the directivities of the radiation field and the energy distribution over different modes. The directivities of the radiation fields are known to have peculiar shapes that depend on the intimate coupling of all wave modes at the interface $x = 0$ [9]. Non-exact solutions might therefore influence the nature of the predicted transition radiation field.

Table 1. Material properties of layers 1 and 2.

	Youngs modulus [MPa]	Poisson's ratio	Material density [kgm^{-3}]
Layer 1	50	0.3	1700
Layer 2	70	0.4	1700

To illustrate the match in the interface conditions, we use the example of a load (F = 10 kN) moving over relatively soft soil of thickness L = 20 m, with a transition to slightly stiffer soil (for material parameters, see Table 1), and a load velocity V = 50 ms^{-1}, which is smaller than the body-wave velocities and the Rayleigh wave velocities of both layers to ensure that the load does not radiate waves while moving over homogeneous soil.

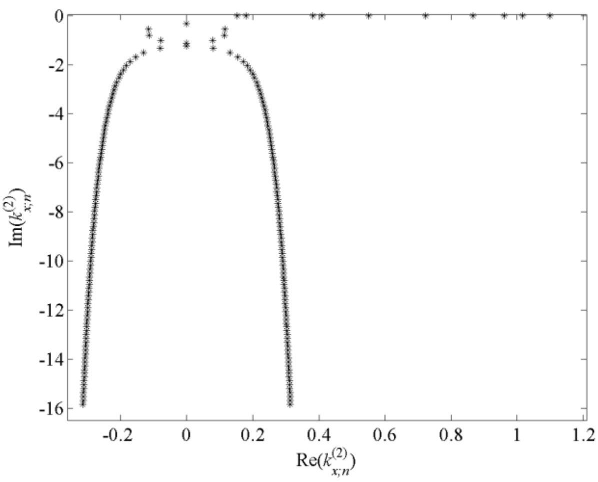

Figure 2. Location of incorporated roots $k_{x;n}^{(2)}$ for layer 2.

We calculated the modal horizontal wavenumbers $k_{x;k}^{(1)}$ and $k_{x;n}^{(2)}$ for a single frequency, f = 20 Hz. We incorporated all roots in the complex plane up to $\mathrm{Im}\left(k_{x;k}^{(1)}, k_{x;n}^{(2)}\right) = -16$, giving M_1 = 205 and M_2 = 203 roots for the left and right layers, respectively. Most of them are located in the interior of the complex plane, as can be seen in Figure 2, where the roots for layer 2 are depicted (the corresponding figure for layer 1 looks very similar); the layers have only 12 and 10 real-valued roots, respectively, and only a few imaginary ones. The largest real-valued roots correspond to the Rayleigh wave at the free surface, and their values are almost the same as that provided by the true Rayleigh root (related to a half-space). The free fields were then computed using the difference in eigenfields (Section 2).

For an increasing amount of incorporated roots, the horizontal interface displacements are depicted in Figures 3 – 6 for f = 20 Hz. The absolute value of the difference in free fields (black line) and that of the difference in eigenfields (red line) are shown; i.e., the left- and right-hand sides of the third line of Eq. (8).

In Figure 3, only the real-valued roots are incorporated in the computation. 15 additional roots are included for both layers (starting from the real axis, with decreasing imaginary part for the successively included roots) in Figure 4, while Figure 5 includes 35 more roots and Figure 6 is the result with all roots M_1 = 205 and M_2 = 203. It is clear that the fit is not perfect in Figure 3. Incorporating a few imaginary roots and some complex roots seems to make the fit even poorer (Figure 4), which is probably the result of the associated relatively strong oscillations; so, there is no monotonous convergence. In Figure 5, however, the difference becomes smaller, and the convergence is quite good in Figure 6. Incorporating even more roots will certainly improve the result further.

To conclude, the shown results illustrate that the derived solution satisfies the interface conditions at each depth, in principal, and not only a depth-integrated form of them.

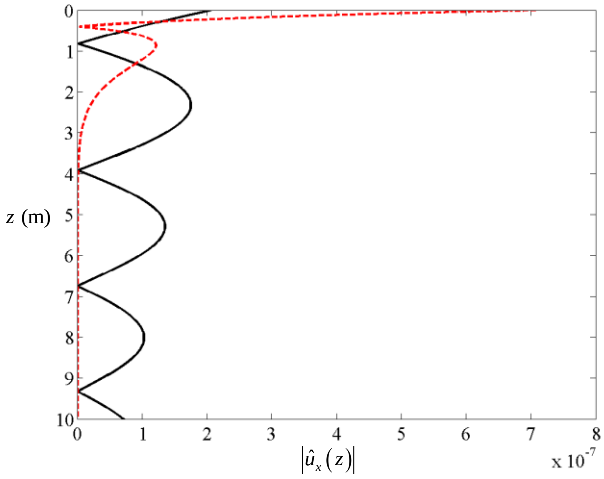

Figure 3. Horizontal displacement at x = 0: magnitudes of difference in free fields (black) and eigenfields (red). Number of roots M_1 = 12, M_2 = 10.

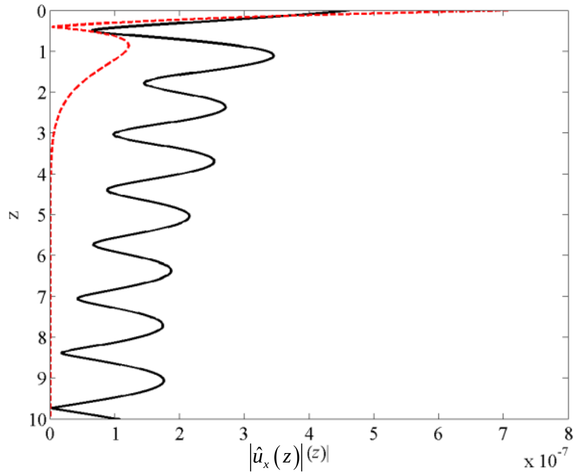

Figure 4. Horizontal displacement at x = 0: magnitudes of difference in free fields (black) and eigenfields (red). Number of roots M_1 = 27, M_2 = 25.

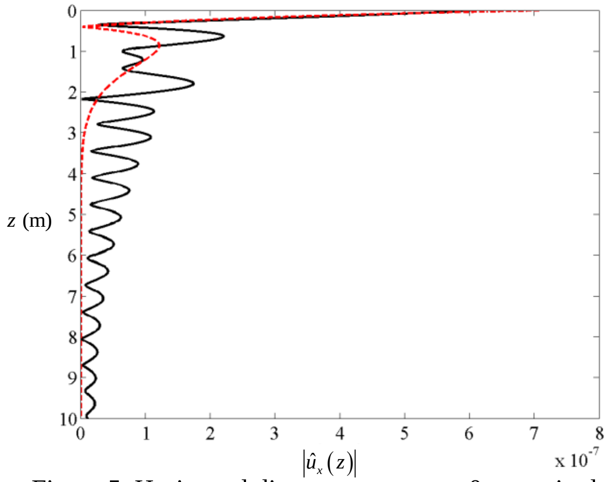

Figure 5. Horizontal displacement at x = 0: magnitudes of difference in free fields (black) and eigenfields (red). Number of roots M_1 = 62, M_2 = 60.

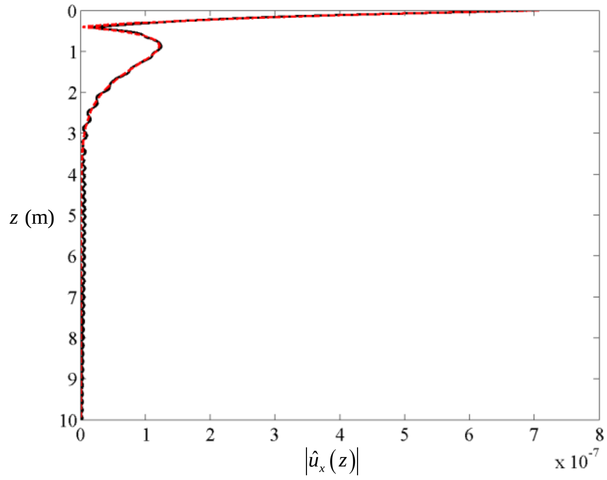

Figure 6. Horizontal displacement at x = 0: magnitudes of difference in free fields (black) and eigenfields (red). Number of roots M_1 = 205, M_2 = 203.

4 CONCLUSIONS AND DISCUSSION

We derived an analytical solution for the problem of a load that moves over the interface of two elastic layers. We showed that the associated transition radiation field, also referred to as the free field as it propagates independently of the load, has the form of a summation over infinitely many guided wave modes, in both layers. Each mode in one layer is coupled to all modes in the other, which constitutes a coupled problem. We showed that the modal coefficients can be computed from the difference of the eigenfields, which move with and are confined to the vicinity of the load, by using orthogonality relations of the modes. Finally, we illustrated that the analytical solution satisfies the interface conditions in the strong sense (not only in an integrated way). The latter finding is important to retain the essential features of the transition radiation field such as directivity and energy distribution over modes.

Regarding the convergence in the interface conditions, we note that more modes are needed to guarantee a match in the stresses than in the displacements (we considered the latter).

This is due to the fact that stresses are related to derivatives of the displacements.

Furthermore, we expect that the solution method described in this paper also works for layered media, perhaps even with structures on top of them (i.e., between the load and the elastic layers, such as a beam), which enables analysis of energy loss for moving trains due to non-uniform subsoil and prediction of the associated ambient vibrations in practical situations.

ACKNOWLEDGMENTS

We thank our colleague Mr. Jeroen Hoving for computational assistance.

REFERENCES

[1] V.L. Ginzburg and V.N. Tsytovich, *Transition Radiation and Transition Scattering*, Hilger, Bristol, 1990.

[2] V.L. Ginzburg and I.M. Frank, Radiation arising from a uniformly moving electron as the electron crosses the boundary between two media. *Journal of Experimental and Theoretical Physics*, 16, 15-30, 1946.

[3] A.I. Vesnitskii and A.V. Metrikine, Transition radiation in one-dimensional elastic systems. *Journal of Applied Mechanics and Technical Physics*, 33, 202-207, 1992.

[4] A.I. Vesnitskii and A.V. Metrikine, Transition radiation in mechanics, *Physics-Uspekhi*, 39, 983-1007, 1996.

[5] Z. Dimitrovová, A general procedure for the dynamic analysis of finite and infinite beams on piece-wise homogeneous foundation under moving loads, *Journal of Sound and Vibration*, 329, 2635-2653, 2010.

[6] K.K. Ang and J. Dai, Response analysis of high-speed rail system accounting for abrupt change of foundation stiffness, *Journal of Sound and Vibration*, 332, 2954-2970, 2013.

[7] J.N. Varandas, P. Hölscher and M.A.G. Silva, Dynamic behaviour of railway tracks on transitions zones, *Computers and Structures*, 89, 1468-1479, 2011.

[8] M.J.M.M. Steenbergen, Physics of railroad degradation: The role of a varying dynamic stiffness and transition radiation processes, *Computers and Structures*, 124, 102-111, 2013.

[9] K.N. van Dalen and A.V. Metrikine, Transition radiation of elastic waves at the interface of two elastic half-planes. *Journal of Sound and Vibration*, 310, 702-717, 2008.

[10] J.W.S. Rayleigh, *The Theory of Sound*, Vol. II, Macmillan and co, London, 1896.

[11] A.T. de Hoop, *Handbook of Radiation and Scattering of Waves*, Academic Press, London, 1995.

[12] K. Aki and P.G. Richards, *Quantitative Seismology*, Freeman and Company, New York, 2002.

[13] J.D. Achenbach, *Reciprocity in Elastodynamics*, Cambridge University Press, Cambridge, 2003.

[14] C.L. Scandrett and C.L. Frenzen, Bi-orthogonality relationships involving porous media, *Journal of the Acoustical Society of America*, 98, 1199-1203, 1995.